J|A|C|S
COMMUNICATIONS

Published on Web 04/08/2006

A Simple Numerical Calculation Correctly Predicts the Observed Size Regime for Growth of Tetrapodal Chalcogenide Nanocrystals

P. John Thomas and Paul O'Brien*

School of Chemistry and School of Materials, The University of Manchester, Oxford Road, Manchester M139PL, U.K.

Received February 3, 2006; E-mail: paul.obrien@manchester.ac.uk

The synthesis of materials with critical dimensions of the order of nanometers is at present an area of intense research.[1] Studies of chalcogenide systems, such as CdSe which can exist in hexagonal (wurtzitic) or cubic (spharelitic) forms as well as polytypical phases, dominate much of this work. In these systems, as exemplified by CdSe, several solution-grown morphologies attract particular attention: (a) close to spherical or oblate proloid particles usually of the hexagonal phase; (b) rods, mostly hexagonal, but not exclusively, growing along the unique 0001 axis of the wurtzite phase; (c) tetrahedra based on close packing and perforce cubic; (d) tetrapodal structures in which hexagonal legs grow on the 111 faces of the above cubic tetrahedron.[2]

Small variations in experimental conditions (for example, concentration) often lead to structures with widely differing morphologies.[2j] A common factor may hence underlie the formation of tetrapods. In all cases, the critical dimensions (other than the lengths of rods or of the legs of the tetrapods) lie in a narrow size range of 2−5 nm for CdSe.[2] These observations have led us to seek an underlying factor governing morphology. We have sought inspiration in the magic numbers approach widely used in understanding the structures of metal and noble gas clusters.[3]

The model is based on a consideration of atomic arrangement in the crystallites at each possible stage during the growth of a tetrapod. The relative energy of different configurations follow the ratio of surface atoms to the total number of atoms. To create a frame of reference, the variation of percentage of surface atoms (SAP) with total number of atoms (T_a) for various commonly observed morphologies is shown in Figure 1 (see Supporting Information for mathematical relations). The calculations were carried out for closed shell structures.

The tetrahedral shape has the highest number of closed shell configurations for a given number of atoms. The tetrahedral shape that seeds tetrapods has the highest SAP and, by implication, the highest energy (among common morphologies). Significantly, the differences in SAP between various morphologies are between 2 and 15%. For example, when the number of atoms, $T_a > \sim 500$, the tetrahedral structure has ∼13 and ∼7% higher SAP than the corresponding regular cuboctahedral and octahedral structures.

The SAP changes accompanying the branched growth of tetrahedral seeds to tetrapods are obtained for *hcp* branches with either triangular or hexagonal shapes. The branches were assumed to grow as is experimentally observed out of a triangular face on the tetrahedron. The number of atoms in *a* and *b* close-packed layers for the triangular branch are dependent on the number of atom layers (N) in the tetrahedron in the following way:

$$a \text{ layer} = [N(N+1)]/2;\ b \text{ layer} = [(N-1)N]/2$$

For the hexagon-shaped branch, the number of close-packed atoms in *a* and *b* layers are obtained in terms of the edge length of the hexagon (D) in units of atoms. The dimensions of the largest

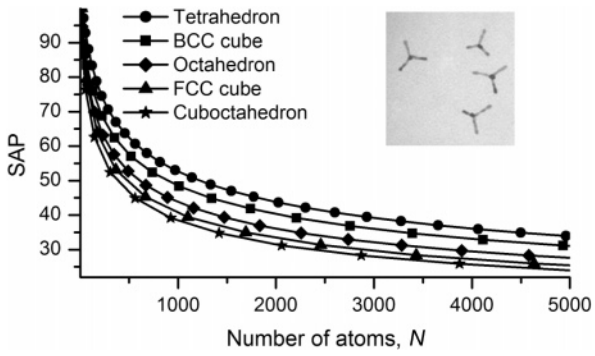

Figure 1. Plot showing the changes in the surface atom percentage (SAP) with increase in the total number of atoms for different crystal morphologies. In the case of a cube, three different close-packing schemes are illustrated. Inset shows a TEM image of CdTe tetrapods with an arm diameter of 4 nm (reproduced with permission from ref 2g).

hexagon that can be grown on a tetrahedron with N atom layers is $D = (N + 2)/3$. Thus

$$a \text{ layer } (D) = \sum_{i=D-1}^{i=2D-1} i + \sum_{j=D}^{j=2D-2} j;$$

$$b \text{ layer } (D) = \sum_{i=D-1}^{i=2D-2} \mathrm{i} + \sum_{j=D}^{j=2D-3} j$$

The above expressions are valid when $D \geq 2$. To identify the surface atoms, the atoms shadowed by an over-layer were identified using the following expressions for triangular branches:

$$a_{\text{shadow}} \text{ layer} = [(N-4)(N-3)]/2;$$

$$b_{\text{shadow}} \text{ layer} = [(N-3)(N-2)]/2$$

For hexagonal branches

$$a_{\text{shadow}} \text{ layer}(D) = a \text{ layer}(D-1);$$

$$b_{\text{shadow}} \text{ layer}(D) = b \text{ layer}(D-1)$$

Subtraction of the shadowed atoms from the total atoms following the addition of the respective over-layer yields the number of surface atoms.

The change in SAP accompanying the growth of initial atom layers of four hexagonal branches from a cubic tetrahedral seed is shown in Figure 2. Perhaps, contrary to intuition, the onset of branching leads to a dramatic lowering in the number of surface atoms compared to growing another layer on the tetrahedral seed. A similar change accompanies the growth of the triangular branch (see Supporting Information, Figure S1). The lower SAP gives the branched structure a lower internal energy (high lattice energy). The structures with the above atomic arrangements are far more

10.1021/ja060825u CCC: $33.50

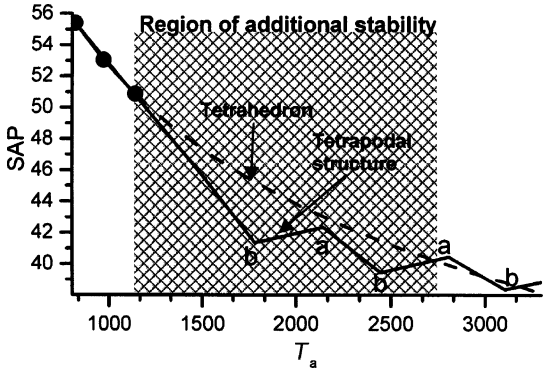

Figure 2. Plot showing the changes in the surface atom percentage (SAP) accompanying the growth of four hexagonal branches. The dotted line represents the SAP profile that the seed would have adopted if branching had not taken place. The atom layers (a and b) are marked in the curve corresponding to the branched structure. For the purpose of calculations, only anions were counted. The CdSe lattice of either structure is made of close-packed anionic layers.

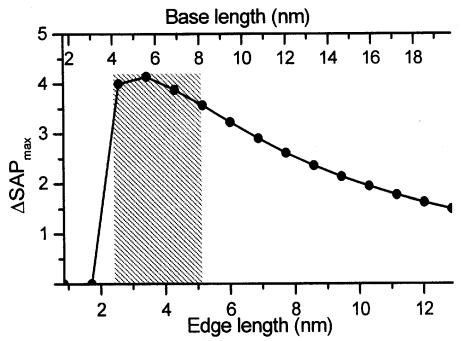

Figure 3. Plot showing changes in the maximum difference in the surface atom percentage (ΔSAP_{max}) between the tetrahedron and the corresponding structures with four hexagonal branches grown from a CdSe seed. The edge length refers to the edge length of the hexagon; the base length pertains to the length of the tetrahedral face from which the branch grows. The size regime for experimentally obtained tetrapods is shaded.

likely to persist in solution by virtue of its lower energy than a tetrahedron with similar number of atoms.

The initial fall in SAP for a tetrapod is strongly dependent on the number of atoms in the tetrahedron. To compare branches originating at different points, each point is associated with ΔSAP_{max}, the maximum difference in the SAPs of branched and unbranched structures with the same number of atoms. A size can be assigned to the number of atoms in the seed and the branch based on the lattice constants of CdSe. ΔSAP_{max} values for hexagonal branches of different diameters are shown in Figure 3 (see Supporting Information, Figure S2). A strong dependence with size is seen in both cases. In the case of hexagonal branches, a maximum gain in SAP of 4.1 is seen when the diameter of the branch (edge length) is 3.5 nm. The gain in SAP diminishes beyond this point. In the case of triangular branches, a more substantial gain of 8.3% is seen, accompanying a broad peak with a maximum in the range of 2−4 nm. The size regime indicated as favorable by SAP gain (shaded area, Figure 3) reproduces very well the size regime in which tetrapods are experimentally obtainable.

The above calculations suggest that branching in semiconductor nanocrystals is driven by minimizing the number of surface atoms and consequently lowering internal energy or maximizing lattice energy. The idea explains why a wide variety of precursors without any templates can grow into these branched structures. One common observation concerning the tetrapodal growth is the necessity of maintaining a high precursor concentration during growth. We speculate that such conditions are necessary to create the high-energy tetrahedral seed that subsequently grow into tetrapods. The unit cell dimensions for zinc blende CdS, CdSe, and CdTe are 0.582, 0.605, and 0.648 nm, respectively. One would expect on the basis of this growth model that the lateral dimensions of the experimentally obtained rods and tetrapods for all these materials would be similar. Indeed, experimentally obtained rods and tetrapods of these material fall in the same size regime, despite a rich diversity in precursors and conditions employed for growth of these structures. The branching of tetrapods to yield hyper-branched structures[4] and dendrites could well be governed by SAP gain.

Several other studies suggest that growth in nanodimensional systems is governed by the need to conserve the number of surface atoms.[3,5] Tetrahedral seeds condense to form multiply twinned nanocrystals driven by the need to maintain a lower SAP.[5d] Configurations with the minimum number of surface atoms are responsible for the stability associated with "magic number" clusters. Such geometric shell effects are observed in gas phase mass spectroscopic studies of metals, semiconductors, and inert gases.[3,5] The gain, measured in terms of SAP, that governs these structures is very similar to that in Figure 3.

The agreement between the size regimes predicted by the calculation and the dimensions of experimentally obtained tetrapods is striking. Therefore, it seems likely that, not withstanding other steps in the growth process, the formation of the low-energy branched structures is a very important step governing the formation of tetrapods. In light of the above observations, we are carefully examining the various steps leading to the growth of nanocrystals into other shapes.

Acknowledgment. The authors thank the University of Manchester for funding this research.

Supporting Information Available: Table showing equations used to derive Figure 1. Plots similar to Figures 2 and 3, showing changes in SAP and ΔSAP_{max} for triangular branches. This material is available free of charge via the Internet at http://pubs.acs.org.

References

(1) (a) Trindade, T.; O'Brien, P.; Pickett, N. L. *Chem. Mater.* **2001**, *13*, 3843−3858. (b) Pickett, N. L.; O'Brien, P. *Chem. Rec.* **2001**, *1*, 467−479.

(2) (a) Manna, L.; Scher, E. C.; Alivisatos, A. P. *J. Am. Chem. Soc.* **2000**, *122*, 12700−12706. (b) Christian, P.; O'Brien, P. *Chem. Commun.* **2005**, 2817−2819. (c) Bunge, S. D.; Krueger, K. M.; Boyle, T. J.; Rodriguez, M. A.; Headley, T. J.; Colvin, V. L. *J. Mater. Chem.* **2003**, *13*, 1705−1709. (d) Peng, Z. A.; Peng, X. *J. Am. Chem. Soc.* **2002**, *124*, 3343−3353. (e) Nann, T.; Riegler, J. *Chem.—Eur. J.* **2002**, *8*, 4791−4795. (f) Thoma, S. G.; Sanchez, A.; Provencio, P. P.; Abrams, B. L.; Wilcoxon, J. P. *J. Am. Chem. Soc.* **2005**, *127*, 7611−7614. (g) Manna, L.; Milliron, D. J.; Meisel, A.; Scher, E. C.; Alivisatos, A. P. *Nat. Mater.* **2003**, *2*, 382−385. (h) Pang, Q.; Zhao, L. J.; Cai, Y.; Nguyen, D. P.; Regnault, N.; Wang, N.; Yang, S. H.; Ge, W. K.; Ferreira, R.; Bastard, G.; Wang, J. N. *Chem. Mater.* **2005**, *17*, 5263−5267. (i) Yu, W. W.; Wang, Y. A.; Peng, X. *Chem. Mater.* **2003**, *15*, 4300−4308. (j) Li, Y.; Li, X.; Yang, C.; Li, Y. *J. Mater. Chem.* **2003**, *13*, 2641−2648. (k) Jun, Y.-W.; Lee, S.-M.; Kang, N.-J.; Cheon, J. *J. Am. Chem. Soc.* **2001**, *123*, 5150−5151. (l) Peng, X. *Adv. Mater.* **2003**, *15*, 459−463. (m) Ascencio, J. A.; Santiago, P.; Rendon, L.; Pal, U. *Appl. Phys.* **2004**, *A78*, 5−7. (n) Peng, Z. A.; Peng, X. *J. Am. Chem. Soc.* **2001**, *123*, 1389−1395.

(3) Martin, T. P. *Phys. Rep.* **1996**, *273*, 199−241.

(4) (a) Milliron, D. J.; Hughes, S. M.; Cui, Y.; Meisel, A.; Manna, L.; Li, J.; Wang, L.-W.; Alivisatos, A. P. *Nature* **2004**, *430*, 190−195. (b) Kanaras, A. G.; Sönnichsen, C.; Liu, H.; Alivisatos, A. P. *Nano Lett.* **2005**, *5*, 2164−2167.

(5) (a) Naher, U.; Zimmermann, U.; Martin, T. P. *J. Chem. Phys.* **1993**, *99*, 2256−2260. (b) Allpress, J. G.; Sanders, J. V. *Aust. J. Phys.* **1970**, *23*, 23−36. (c) Kumar, V. *Prog. Cryst. Growth Char.* **1997**, *34*, 95−131. (d) Duff, D. G.; Curtis, A. C.; Edwards, P. P.; Jefferson, D. A.; Johnson, B. F. G.; Logan, D. E. *J. Chem. Soc., Chem. Commun.* **1987**, 1264−1266.

JA060825U